Measurement of LAGEOS-2 Rotation by SLR Observations

G. Bianco - *Agenzia Spaziale Italiana, CGS - Matera*
M. Chersich - *FMR Spazio S.r.l.*
R. Devoti, V. Luceri - *Telespazio S.p.A., CGS - Matera*
M. Selden - *Honeywell Technology Solution Inc.*

The unprecedented single shot precision of the newborn Matera Laser Ranging Observatory (MLRO), that can reach a scattering down to a few millimeters on LAGEOS orbit, discloses new chances in studying the high frequency dynamics.
In this work we discuss the cause of the high frequencies noticed since the testing phase of the MLRO system (see figure 1). There are sufficient theoretical and experimental evidences to interpret those signals as rotational signatures of the spinning satellite and the first quantitative results we obtained indicate a rotation period of 23.5 s on May 31, 2000.

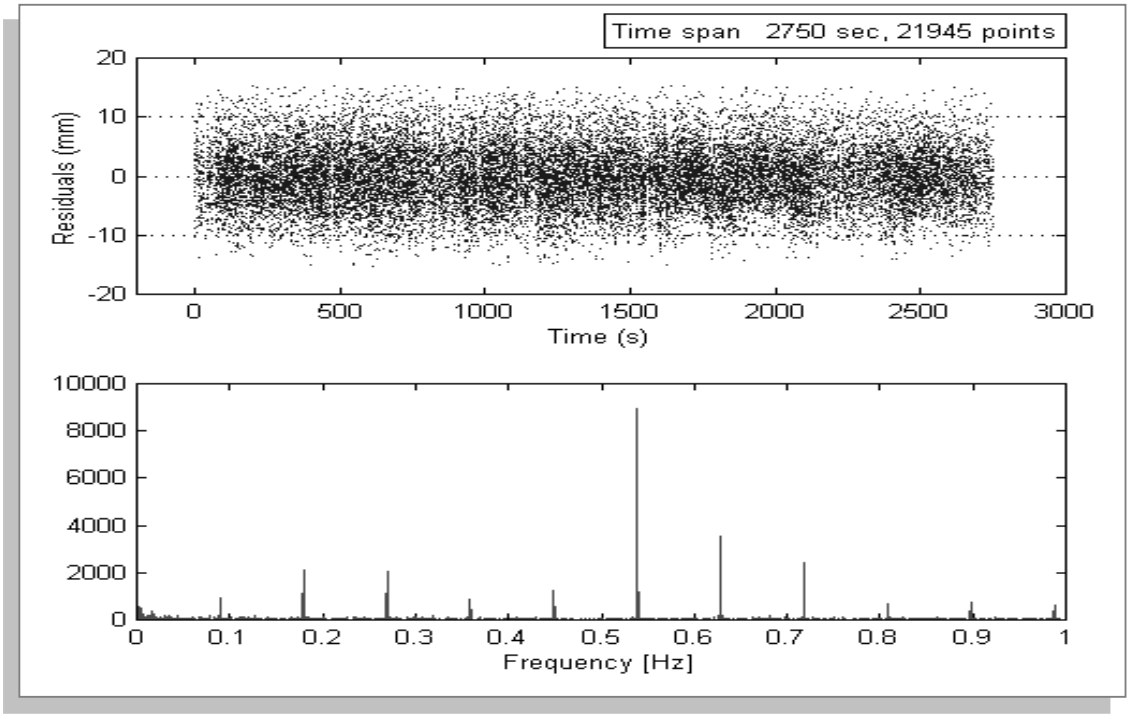

Figure 1: signatures in LAGEOS-2 range residuals spectrum.

The goal of this paper is to explain the physics underlying these signatures and to set up a feasibility study for a direct SLR observation of both the rotation period of LAGEOS-2 and its spin axis orientation.

To do so we have accurately modeled the entire path of the transmitted pulse (see figure 2), and the transformations it undergoes during the flight, from the reflection by LAGEOS-2 reflectors array to the signal processing of the detection apparatus.
We produced simulations of range observable and compared the spectra of the residuals to the experimental data gathering important results.

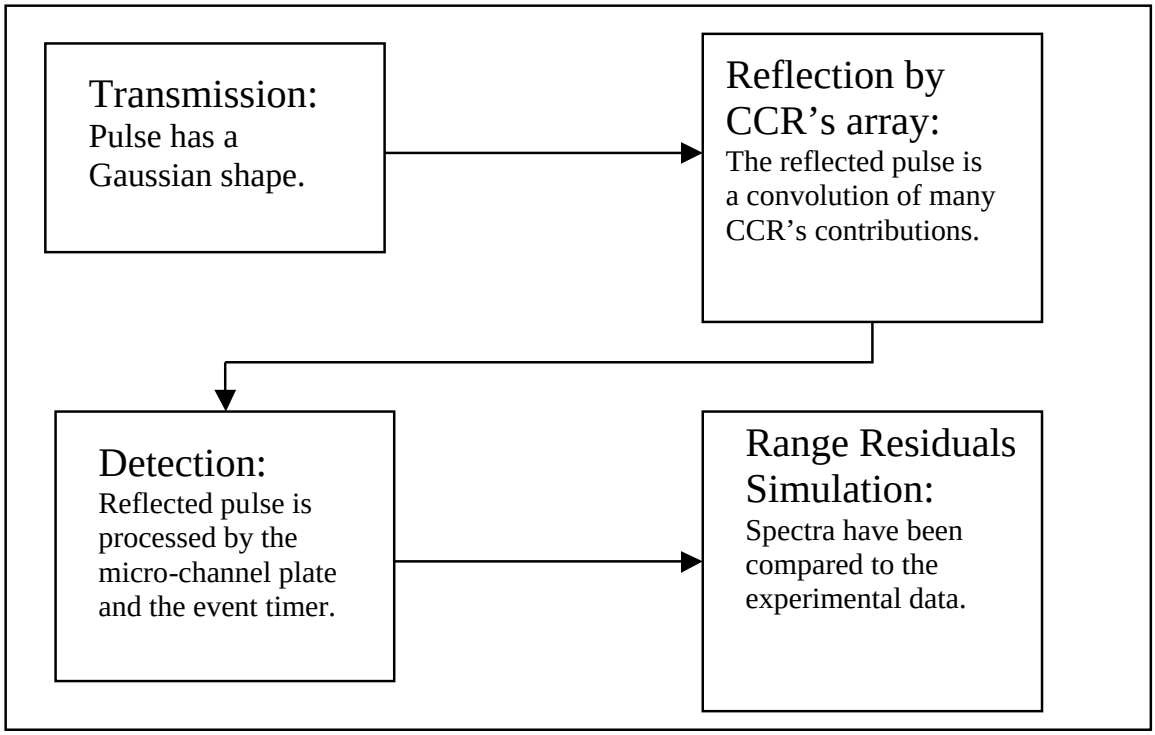

Figure 2: signal processing scheme.

Each reflector contributes to the total reflected light with a Gaussian signal whose integral is proportional to the cross section of the CCR and retarded by twice the flight time from the boundary of the satellite to the center of the reflecting surface (see figure 3). The reflected energy is proportional to a function of the incidence angle:

$$2a^2\rho\,[\arcsin\mu-\sqrt{2}\mu\tan r]\cos i$$

$$r=\arcsin(\frac{\sin i}{n})$$

$$\mu=\sqrt{1-2\tan^2 r},$$

where i is the incidence angle, r the refraction angle, n the refraction index of the cube corner prism, r the efficiency characteristic to account for reflection losses and a the radius of the cube corner aperture.
This function describes not only the geometrical cross-section of the reflector but also its optical characteristics.

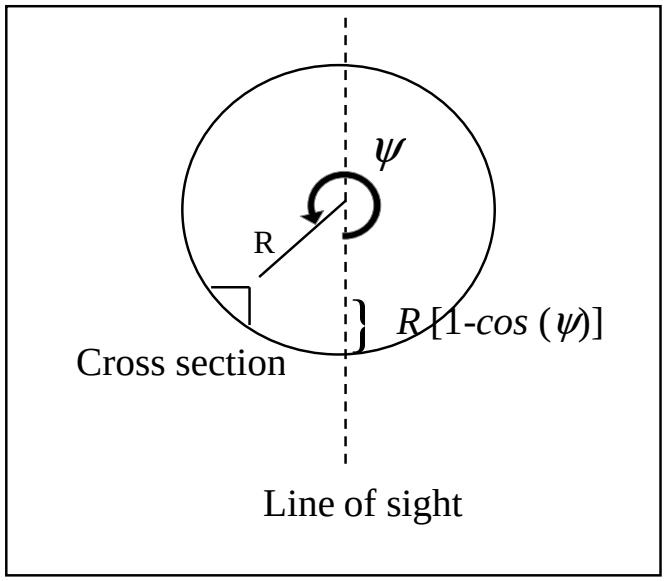

Figure 3: mirror geometrical configuration.

The light impinging on LAGEOS-2 (a 30ps long Gaussian pulse) is the convolution of many CCR's lying at different distances from the observer and having different cross-sections. The reflected pulse is a complex convolution of the active CCR's contributions and is about ten times longer than the transmitted pulse.

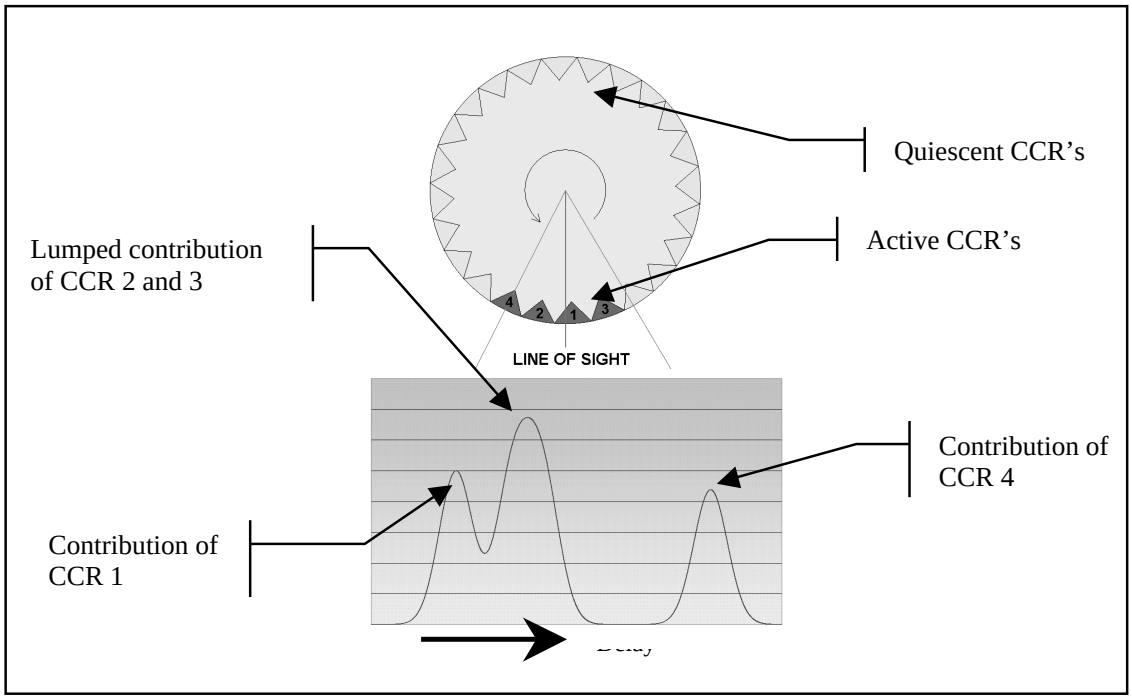

Figure 4: reflected pulse shape.

The upper frame of figure 4 represents the cross section of the equatorial plane of the satellite, showing the arrangement of the CCR's. The lower panel represents the reflected light intensity distribution as a function of time (delay). Only four CCR's, over the 24 composing the ring, contribute to the signal. CCR number 1 is the closest to the observer and its response is minimally delayed.
Given their position, signal delays for CCR 2 and 3 are very close, so that the individual contributions are not separated. Since their optical planes are behind the optical plane of CCR 1, their response is visible after the response of CCR 1. Finally, CCR 4 contributes with another peak, further delayed.
Results similar to the one described here have been observed in the pre-launch optical tests on LAGEOS II (Pre-launch Optical Characterization of the Laser Geodynamic Satellite (LAGEOS-2), P.Minott et al., NASA Tech. Paper 3400, 1993).

The energy contribution of each CCR is a function of the instantaneous light incidence angle and grows sharply whenever the incidence angle becomes smaller than the acceptance angle. As the satellite rotates, the “rising” and “setting” of CCR’s determines the modulation of the total reflected energy and of the signal shape (see figure 5).

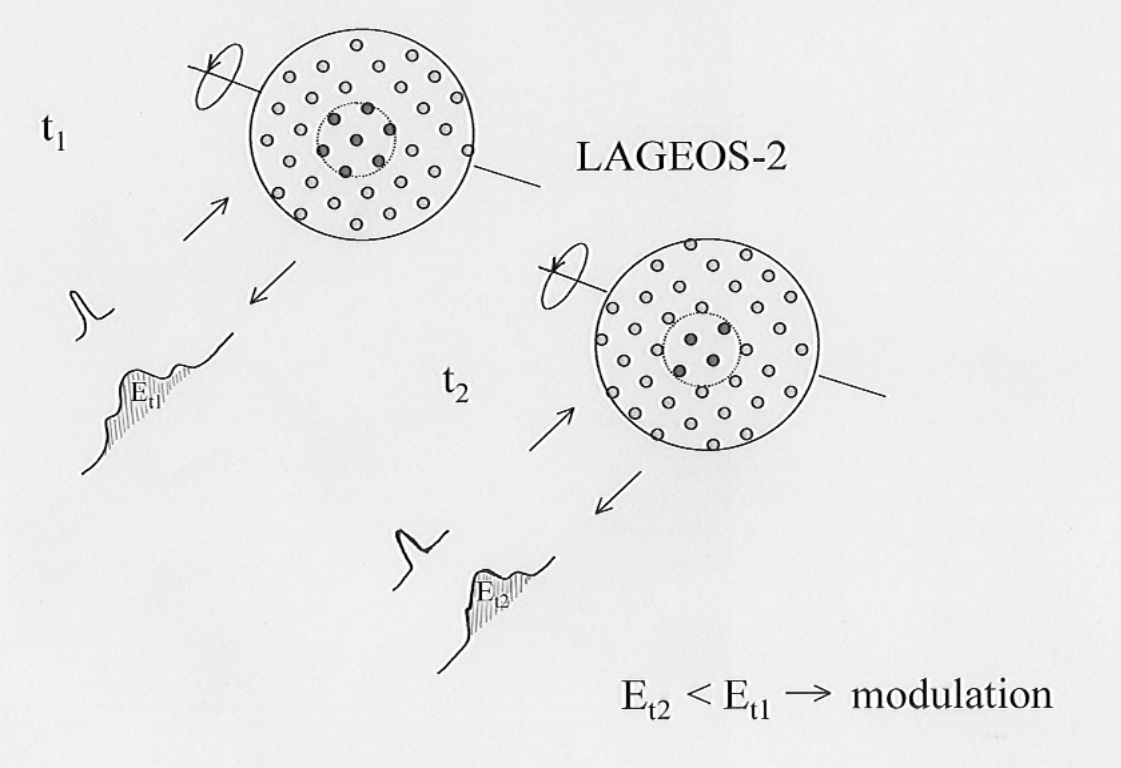

Figure 5: effect of rising and setting of CCR’s on pulse shape.

Observing the satellite equator and performing a spectral analysis upon the simulated range residuals time series we can see strong peaks at 32, 31, 27 and 23 times the rotation fundamental frequency, nominally set to 10s (see figure 6). In fact we have the

same mirrors configuration of the 32 CCR's band every 1/32 revolution and similarly for the other bands.

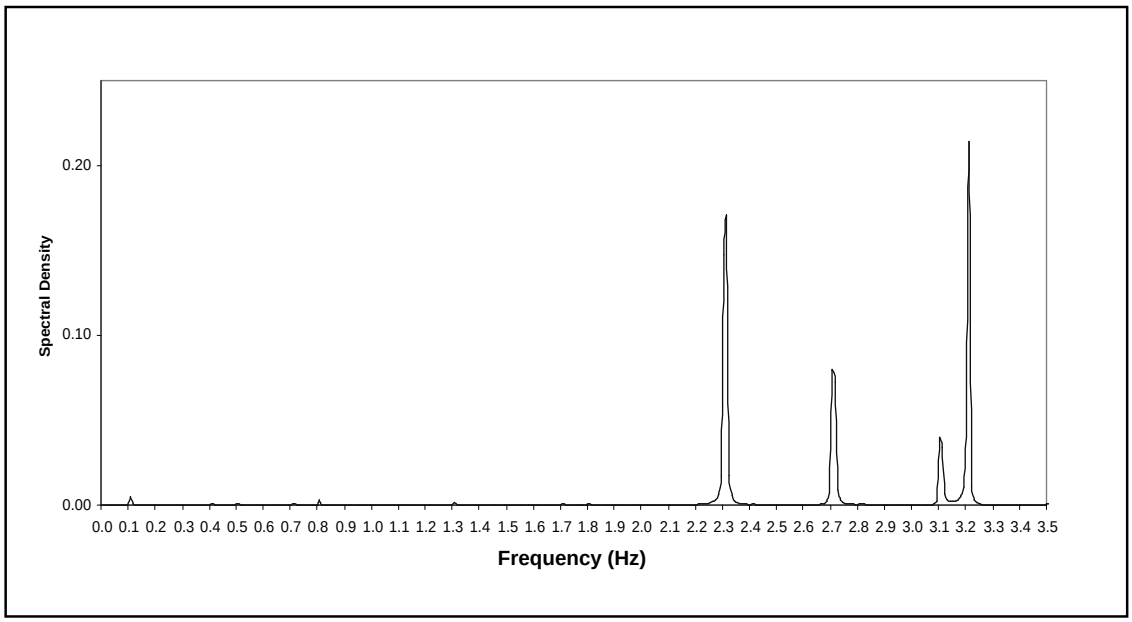

Figure 6: simulated range residuals spectrum (equator view).

Moving towards the Polar Regions, peaks at lower frequencies begin to appear. The modulation disappears completely once the observer aligns itself to the satellite pole (see figure 7).

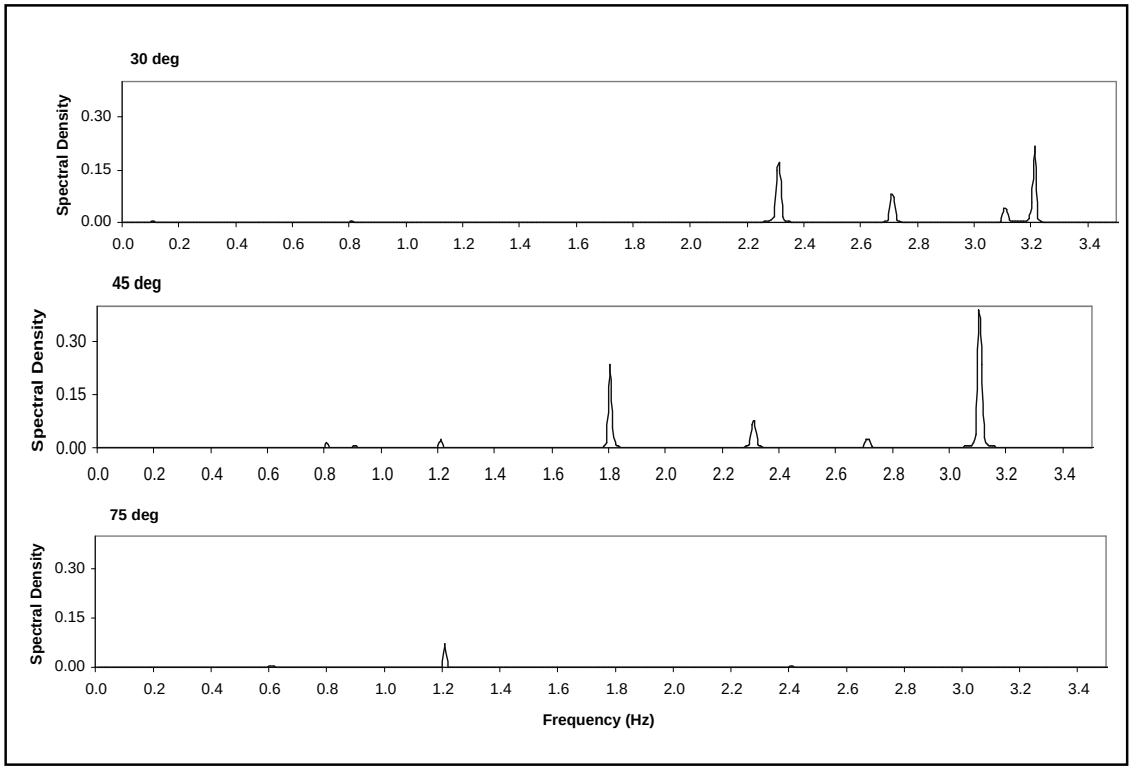

Figure 7: simulated range residuals spectrum (moving towards pole).

In general these spectra look very different respect to the experimental data, where clear uniformly spaced peaks appear at lower frequency, as in the figure below.

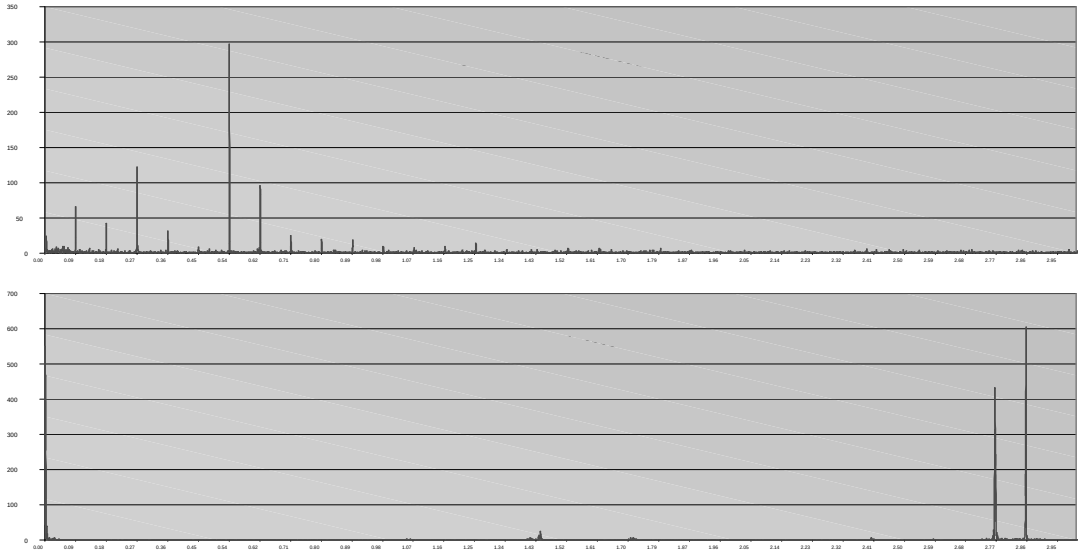

Figure 8: measured vs. simulated range residuals spectra.

These spectra have been computed using the Scargle algorithm for unequally spaced data analysis.
In spite of the satellite motion simulation, the two spectra still look very different. The observed spectrum shows strong peaks at the fundamental frequency and its integer multiples. The simulated spectrum puts in evidence strong peaks at higher frequency harmonics.

At the moment the model is somewhat coarse and we have to further investigate several factors that may affect pulse shape.
The first and most important factor we have to investigate to refine the simulation process is the CCR geometry, which produces a characteristics far-field diffraction pattern depending upon the azimuth of the reflector, i.e. the rotation of the prism in the satellite body, so far neglected.
Second, we have to investigate the effect of the coherent interference when two or more reflectors lie at about the same distance from the observer.
Third, the indetermination of the accuracy of the dihedral offsets between the reflecting surfaces of the cube corner may affect the reflected beam direction. This beam deviation shifts the diffraction pattern at ground affecting the intensity of the received light.

However depending upon different physical processes, all the above-mentioned factors affect, in a different way, the intensity of the pulse reflected by each CCR. This induced us to multiply the response function of each CCR by an arbitrary random number. The result is that every CCR is considered to have a random reflection index (kept constant during the simulation) and this indetermination transfers power from the higher frequencies to the fundamental frequency and its harmonics. By adding this randomization, we reproduce the same frequency distribution as in the experimental data (see figure 9), and the frequency distribution is not affected by the particular choice of random constants, thus confirming that we are not introducing artificial effects.

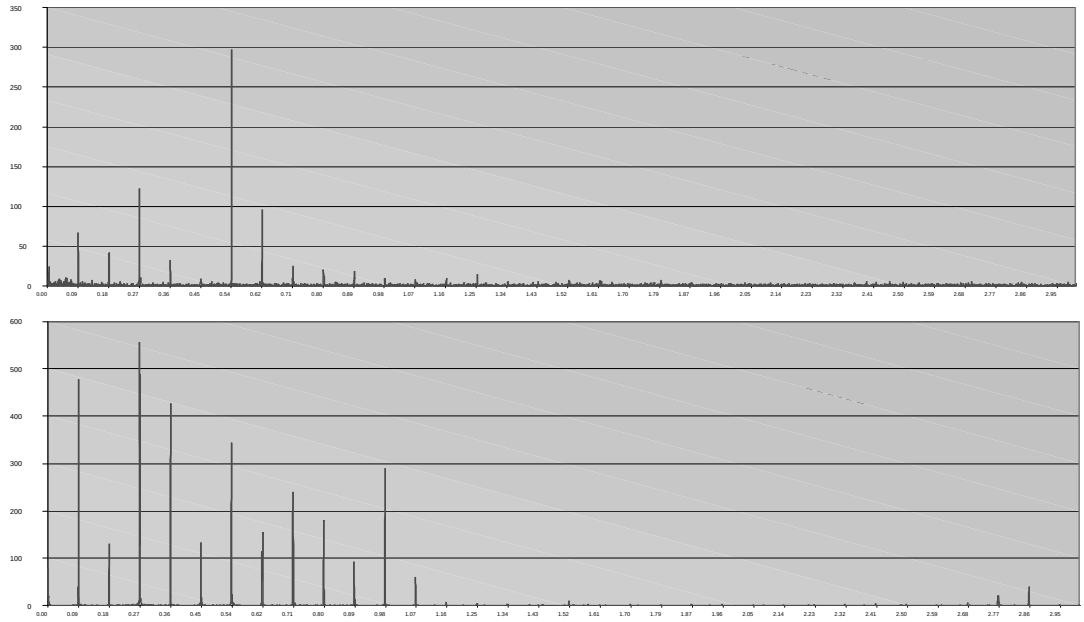

Figure 9: measured vs. simulated range residuals spectra (randomization).

Nevertheless, the amplitudes of the harmonics show a strong dependence from the choice of random constants, as in the figure below.

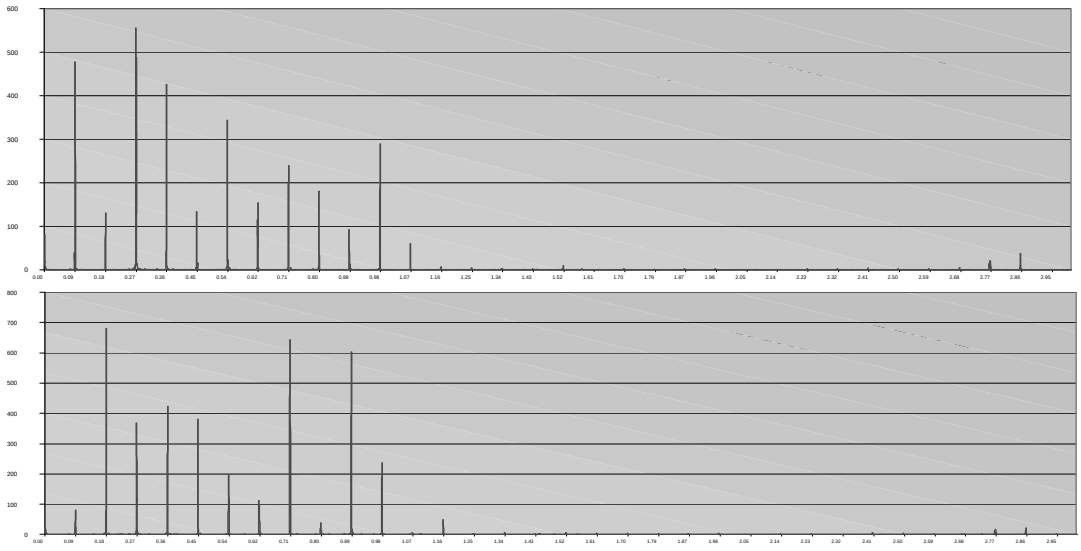

Figure 10: two different choices of random constants.

The orientation of the satellite rotation axis affects the simulated spectra as well (see figure 11). As a consequence we cannot separate the satellite attitude from the CCR geometry until a good modeling of the previously mentioned factors will be performed.

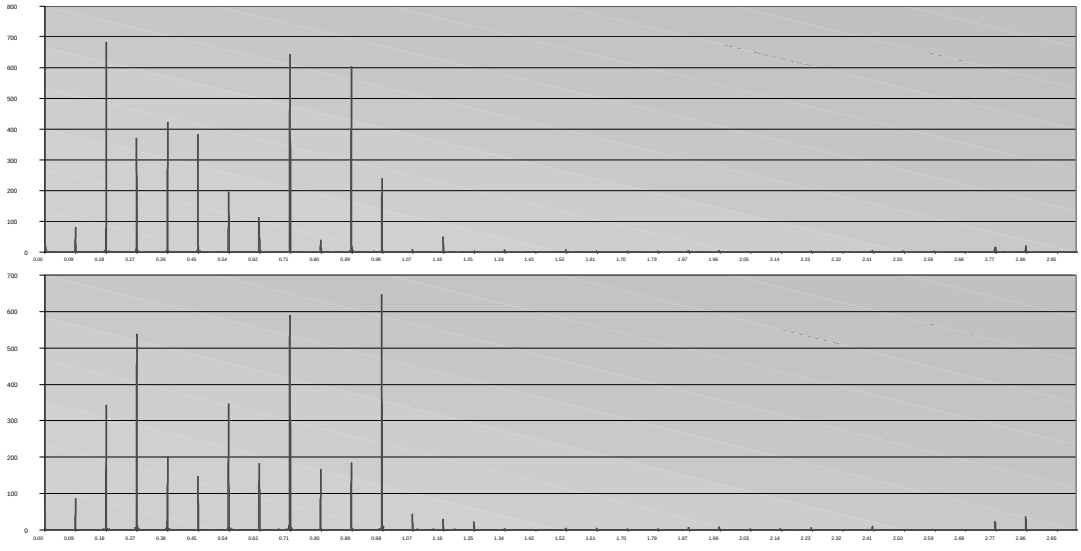

Figure 11: two different choices of axis orientation.

If the model presented here is reasonable, we have a confidence that the first peak of the measured range residuals spectra corresponds to the rotation frequency of LAGEOS-2.
A specific part of software has been developed to find the first peak frequency. The data in figure 12 have been taken from the MLRO station test in Greenbelt-USA (from August 21st to October 24th, 19 passes). The points have been placed in a logarithmic vertical scale (according to the Bertotti-Iess model) and a linear regression has been performed. Rotation periods range from 10.4s to 24s, showing an evident down-spinning of LAGEOS-2. The foreseen rotation period of LAGEOS-2 on November 15th is 29.1s. The post-fit RMS is 34.9ms.

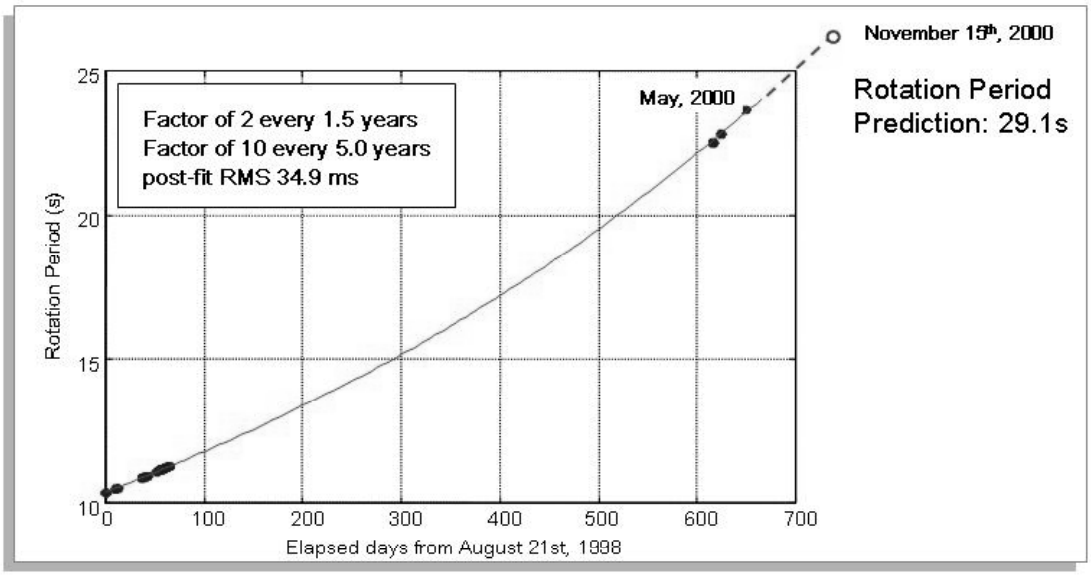

Figure 12: rotation period (s) vs. elapsed days.

The work presented here is by no means complete. The following aspects require further investigation in order to obtain an operative methodology to determine the rotation period and spin axis orientation of LAGEOS-2:

- Precise modeling of the far-field diffraction pattern;
- Coherent interference between cube corners;
- Spreading of the reflected beam due to the cube corners dihedral offsets;
- Effects due to the calibration of the receiver detector (time-walk adjustment);
- Light polarization;
- Atmospheric effects.

Some of them are mere technical points other may unveil methodological difficulties.

This qualitative simulation has shown that if single shot, millimeter accuracy orbital fit range residuals were made available, their power spectra show significant dependence on the rotational parameters even if the orientation of the satellite spin axis is hidden in the amplitude distribution of the spectra and cannot be discovered using range residual observations.
This study suggests that the use of a streak camera, capable to measure the fine details of the returned pulse, may lead to a better determination of the satellite attitude and rotation. We therefore envisage a creation of a stable routinely measurement program based on these data.

References

Bertotti, B. and L. Iess,
The rotation of LAGEOS,
J. Geophys. Res., 96(B2), 2431-2440, 1991.

Bianco, G., V. Luceri and M. D. Selden,
Possible evidence of LAGEOS' rotational period by frequency analysis of MLRO SLR full-rate residuals time series,
WEB page at the URL http://www.asi.it, path:
/00HTL/eng/asicgs/geodynamics/mlro1stres.html,
December 1998.

Ciufolini, I.,
Measurement of the Lense-Thirring drag on high altitude, laser-ranged artificial satellites,
Phys. Rev. Lett., 56, 278-281, 1986.

Currie, D., K. Kissel, P. Avizonis and D. Wellnitz,
On the Dynamics of the LAGEOS-I Spin Vector: High Precision Direct Observations and Comparisons to Theoretical Modeling,
Dynamics and Astrometry of Natural and Artificial Celestial Bodies,
eds. I.M. Wytrzyszczak, J.H. Lieske and R.A. Feldman, pp. 341-346,
Kluwer Academic Publishers, 1997.

Farinella, P., D. Vokrouhlicky and F. Barlier,
The rotation of LAGEOS and its long-term semimajor axis decay: a self-consistent solution,
J. Geophys. Res., 101(B8), 17,861-17,872, 1996.

Minott, P. O., T. W. Zagwodzki, T. Varghese and Michael Selden, Prelaunch Optical Characterization of the Laser Geodynamic Satellite (LAGEOS 2),
NASA Tech. Paper 3400, September 1993.

Rubincam D. P.,
LAGEOS Orbit Decay Due to Infrared Radiation From Earth,
J. Geophys. Res., 92(B2), 1287-1294, 1987.

Scargle, J. D.,
Studies in astronomical time series analysis. II. Statistical
aspects of spectral analysis of unevenly spaced data,
Ap. J., 263, 835-853, 1982.

Tapley, B. D., B. E. Schutz, R. J. Eanes, J. C. Ries and M. M. Watkins,
Lageos Laser Ranging Contributions to Geodynamics, Geodesy,
and Orbital Dynamics,
Contributions of Space Geodesy to Geodynamics:
Earth Dynamics, Geodyn. Series Vol. 24, edited by
D. E. Smith and D. L. Turcotte, pp. 147-173, Washington, D.C., 1993.